

Multiscale Adaptive Conflict-Balancing Model For Multimedia Deepfake Detection

Zihan Xiong

2022090905007@std.uestc.edu.cn

University of Electronic Science and Technology of China
Chengdu, Sichuan, China

Lei Chen

202322090726@std.uestc.edu.cn

University of Electronic Science and Technology of China
Chengdu, Sichuan, China

Xiaohua Wu*

wuxh@uestc.edu.cn

University of Electronic Science and Technology of China
Chengdu, Sichuan, China

Fangqi Lou

202422090730@std.uestc.edu.cn

University of Electronic Science and Technology of China
Chengdu, Sichuan, China

Abstract

Advances in computer vision and deep learning have blurred the line between deepfakes and authentic media, undermining multimedia credibility through audio-visual forgery. Current multimodal detection methods remain limited by unbalanced learning between modalities. To tackle this issue, we propose an Audio-Visual Joint Learning Method (MACB-DF) to better mitigate modality conflicts and neglect by leveraging contrastive learning to assist in multi-level and cross-modal fusion, thereby fully balancing and exploiting information from each modality. Additionally, we designed an orthogonalization-multimodal pareto module that preserves unimodal information while addressing gradient conflicts in audio-video encoders caused by differing optimization targets of the loss functions. Extensive experiments and ablation studies conducted on mainstream deepfake datasets demonstrate consistent performance gains of our model across key evaluation metrics, achieving an average accuracy of 95.5% across multiple datasets. Notably, our method exhibits superior cross-dataset generalization capabilities, with absolute improvements of 8.0% and 7.7% in ACC scores over the previous best-performing approach when trained on DFDC and tested on DefakeAVMiT and FakeAVCeleb datasets.

CCS Concepts

• **Computing methodologies** → **Machine learning**; **Computer vision**; **Machine learning approaches**.

Keywords

Multimedia machine learning, Video-Audio Deepfake, Multimodal Fusion, Contrastive Learning

*Corresponding author

Permission to make digital or hard copies of all or part of this work for personal or classroom use is granted without fee provided that copies are not made or distributed for profit or commercial advantage and that copies bear this notice and the full citation on the first page. Copyrights for components of this work owned by others than the author(s) must be honored. Abstracting with credit is permitted. To copy otherwise, or republish, to post on servers or to redistribute to lists, requires prior specific permission and/or a fee. Request permissions from permissions@acm.org.
ICMR '25, Chicago, IL, USA

© 2025 Copyright held by the owner/author(s). Publication rights licensed to ACM.
ACM ISBN 979-8-4007-1877-9/2025/06
<https://doi.org/10.1145/3731715.3733403>

ACM Reference Format:

Zihan Xiong, Xiaohua Wu, Lei Chen, and Fangqi Lou. 2025. Multiscale Adaptive Conflict-Balancing Model For Multimedia Deepfake Detection. In *Proceedings of the 2025 International Conference on Multimedia Retrieval (ICMR '25)*, June 30-July 3, 2025, Chicago, IL, USA. ACM, New York, NY, USA, 9 pages. <https://doi.org/10.1145/3731715.3733403>

1 INTRODUCTION

Lately, with the rapid development of computer vision and deep learning, it has become possible to create complex deepfake videos, especially multimodal audio-video deepfakes which have become increasingly rampant[4, 19, 37]. Audio-video deepfake information spreads rapidly on the internet, not only infringing on personal privacy but also potentially causing social security issues. However, research targeting this form of forgery remains relatively scarce, mostly focusing on unimodal detection without fully utilizing multimodal information[32, 44], creating significant pain points in areas such as cybersecurity, authentication, and media content review. Therefore, there is an urgent need to develop a detection method that fully balances and utilizes multimodal information to combat these audio-video deepfakes.

Indeed, research on multimodal deepfake detection is gradually gaining attention[7, 28, 42]. Existing modal fusion methods, however, remain overly simplistic, often employing linear concatenation that ignores the importance allocation and equally combines features from each modality[26]. This strategy fails to adequately explore and utilize the potential complementary information between individual modalities and lacks the exploitation of deeper information. During the fusion process, the lack of in-depth feature interaction and cross-modal relationship modeling may lead to bias towards one modality, thereby affecting the overall detection performance. Some modal fusion methods introduce attention mechanisms[3, 47], which can dynamically adjust weights based on the importance of different modalities, thus better capturing the relevance and differences among multimodal features and effectively enhancing the comprehensive utilization capability of multimodal information, improving the overall detection performance. The aforementioned methodologies predominantly employ contrastive learning to reduce the distance between similar samples while increasing the separation between dissimilar ones. This approach facilitates a more discriminative representation of features in different modalities, thereby allowing the model to learn

comprehensive and balanced characteristics[30, 39, 41]. However, even after applying contrastive learning, clustering information can be further exploited to enhance feature representation.

Moreover, incorporating contrastive loss and classification loss for both single-modal and multimodal scenarios introduces complexities during backpropagation, particularly concerning gradient conflicts. If gradients from different modalities conflict during training, it may impede the effective integration of multimodal information, leading to suboptimal performance. Therefore, it is imperative to investigate a more holistic and efficient method for multimodal fusion that maintains equilibrium throughout the entire training process, we aim to develop a robust multimodal fusion framework that effectively integrates information from various modalities, thereby improving the overall performance and reliability of deepfake detection systems.

Inspired by the above analysis, we propose a multimodal contrastive learning method aimed at reducing biased emphasis during multimodal fusion and addressing non-negligible modality information conflicts when detecting multimodal deepfakes. As shown in Figure 1, we first extract modality features from audio and video, and these two modality features undergo clustering through category and authenticity contrastive learning, generating two sets of weights to guide modality fusion. Then, single-modality features are deeply extracted to obtain finer-grained features, which are secondarily fused with the initial fusion information, allowing single modalities to learn global multimodal information. After interacting with shallow and deep fusion information, the final fused feature information is obtained. Finally, we design an orthogonalization-multimodal pareto module to maintain single-modality information while resolving gradient conflicts caused by loss functions with different optimization objectives in audio and video encoders. The main contributions of this paper are summarized as follows:

- We design a modality-specific and cross-modal contrastive learning module with adaptive temperature regulation based on the authenticity of audio and video (which performs contrastive clustering processing in a unified mapping space) subsequently using video and audio information to generate weight parameters for modality fusion, optimizing the fusion effect of multimodal information.
- To address gradient conflicts between unimodal and multimodal processes, we propose an orthogonalization-multimodal Pareto optimization module. This approach not only resolves conflicts but also promotes diversity and complementarity in modality fusion.
- Through experiments, we demonstrate that our designed model achieves optimal performance with accuracies of 96.8% on DefakeAVMiT, 91.7% on FakeAVCeleb, and 97.9% on DFDC, and multiple ablation experiments fully illustrate the effectiveness of the modules we have designed.

2 RELATED WORK

2.1 Unimodal Deepfake Detection Methods

The rapid advancement of synthetic media has significantly compromised cybersecurity frameworks, identity authentication systems, and content moderation protocols. Contemporary detection

methodologies are primarily categorized into two paradigms: unimodal approaches that independently analyze individual video sequences for facial inconsistencies or audio tracks for synthetic speech patterns, and multimodal frameworks such as audio-visual cross-modal analysis, which leverage inter-modal correlations to achieve superior detection accuracy.

Image Forgery Detection : Advancements in deep learning have spurred the development of CNN-based methods. One such approach[20]introduced a rapid and effective copy-move forgery detection algorithm through hierarchical feature point matching. Another study[25]critically examined the limitations of conventional techniques and explored the efficacy of deep learning methodologies for the detection of forgery. Subsequently, an increasing number of network architectures and modules have emerged [12, 34, 35], exemplified by the introduction of FCD-Net [13], a novel network framework designed to differentiate various types of deepfake facial images with common origins.

Video Forgery Detection : The temporal continuity inherent in videos presents both an aid and a challenge for deepfake detection. To improve the performance of the model, advanced techniques can be employed, such as attention mechanisms[8]or Capsule Networks[27] can be employed. Although these methods operate primarily on static frames, their effectiveness can be enhanced by frame-level score aggregation or using different color spaces as input [14]. Temporal dependencies between frames can be captured using Long Short-Term Memory Networks (LSTM)[33] , thereby improving detection accuracy. In pursuit of enhanced generalization capabilities, hierarchical neural networks were leveraged in [11] to exploit long-term dependencies, integrating attention mechanisms and adversarial training to fortify robustness against compressed videos and novel forgeries.

Audio Forgery Detection : Deepfake audio methodologies predominantly focus on voice conversion [24] and Text-to-Speech (TTS), also known as speech synthesis. Some audio deepfakes involve selectively altering specific segments of original clips using AI technologies while preserving the overall authenticity of the recording, rather than synthesizing entire audio tracks. Current approaches to detecting deepfake audio facts largely focus on analyzing acoustic properties, such as speech patterns, vocal characteristics, and linguistic nuances, to identify anomalies that deviate from natural audio attributes. Furthermore, leveraging aligned video information, such as lip movement synchronization with speech[15], inconsistencies between background environments in videos and spoken content, or discrepancies between audio narratives and video scenarios, can further aid in identifying forged audio.

2.2 Unimodal Bias in Multimodal Deep Learning

The success of multimodal deep learning hinges on the effective integration and utilization of multiple modalities [1, 21, 31]. However, during joint training, certain multimodal networks exhibit a propensity to overly rely on modalities that are easier or faster to learn, thereby neglecting other modalities [2, 22, 36].[38] introduced a gradient analysis-based metric to evaluate unimodal bias within multimodal models. This approach quantifies how much each modality contributes to the final prediction, revealing any

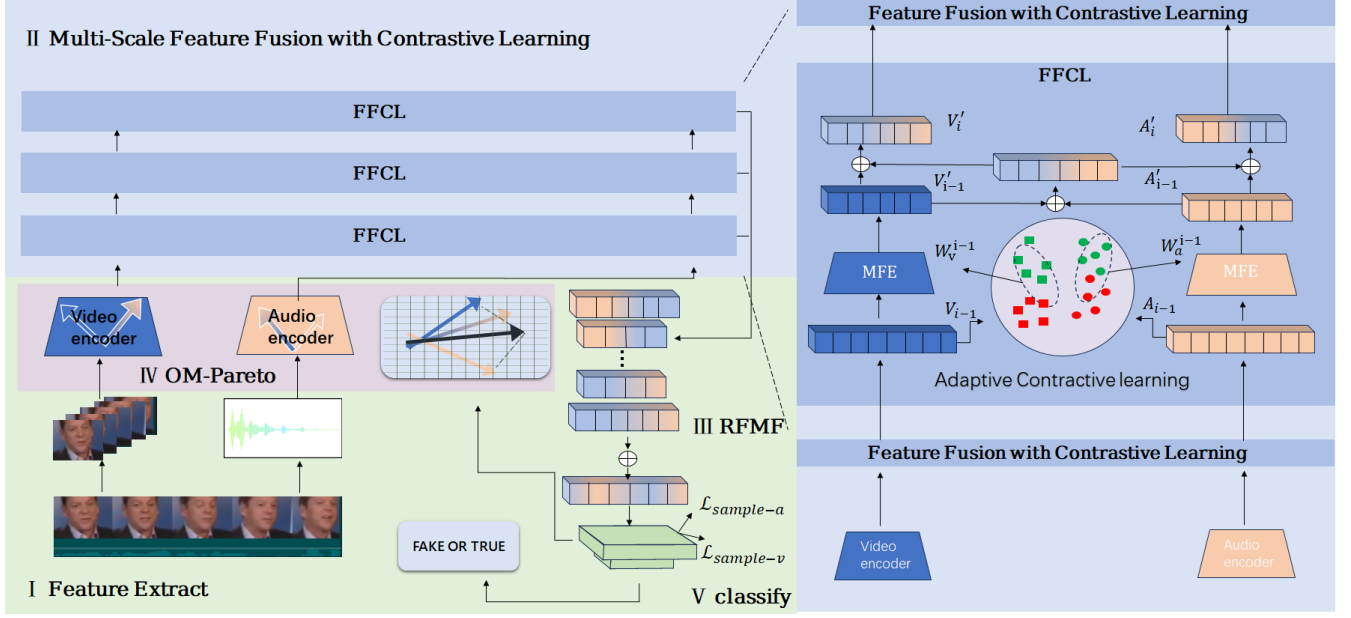


Figure 1: Multiscale Adaptive Conflict-Balancing model for multimedia Deepfake detection deeply balances conflicts and biases among modalities, thereby fully unlocking the potential of intra-modality and inter-modality information. There are five stages in this method: Feature Extract, Multi-Scale Feature Fusion With Contrastive Learning, RFMF, OM-Pareto, Classify

potential biases towards specific modalities.[29] empirically demonstrated that competition among modalities can lead to the neglect of certain modalities. Their findings underscore the importance of balancing contributions from different modalities to ensure comprehensive learning[45, 46].

To address these challenges, our work introduces a learnable contrastive learning framework aimed at facilitating more balanced and holistic feature representation. This method not only aids the model in acquiring a richer and more equitable understanding of the data but also guides modality fusion effectively. Additionally, we employ an Orthogonalization-multimodal Pareto formulation to mitigate conflicts arising from gradient updates across multiple modalities, ensuring that no single modality dominates the learning process.

3 METHOD

We propose a novel Multiscale Adaptive Conflict-Balancing model for multimedia Deepfake detection (MACB-DF) in Figure 1. This model adeptly balances conflicts and biases among modalities, thereby fully unlocking the potential of intra-modality and inter-modality information.

3.1 Feature Extract

The MACB-DF model processes video-audio pairs $(V, A) \sim P$ through two encoders: a video encoder E_v and an audio encoder E_a . For video input V , temporal and spatial information is encoded by E_v via self-attention layers and feed-forward networks, producing a global spatiotemporal video feature $H_v^{(L)}$. Audio processing begins with the STFT of signal A , generating a spectrogram $S(t, f)$ where

t indexes time frames and f denotes frequency. This spectrogram is then projected to Mel-scale using filter banks $\{H_m(f)\}_{m=1}^F$:

$$M(t, m) = \sum_f H_m(f) |S(t, f)|^2 \quad (1)$$

where F is the number of Mel filters. The logarithmic transformation $\log M(t, m)$ is applied to amplify low-energy components. The resulting log Mel-spectrum is encoded by E_a through self-attention mechanisms and feed-forward operations, yielding a global audio feature $H_a^{(L)}$ with temporal dependencies.

3.2 Multi-Scale Feature Fusion With Contrastive Learning

3.2.1 Multi-modal Adaptive Contrast Learning. To facilitate more effective exploitation of the correlations between video and audio by the two single-modal encoders, we employ contrastive learning to align video and audio embeddings. Traditional inter-modality contrastive learning methods, however, often suffer from an inability to fully leverage the intrinsic information within each modality. Moreover, fluctuations in the temperature parameter can significantly impact the gradient of the contrastive loss, leading either to insufficient capture or excessive blurring of detailed information. Additionally, these methods do not make full use of the information post-clustering.

Therefore, we propose *Multi-modal Adaptive Contrast Learning* (MACL). To formalize the contrastive loss from audio to video, we

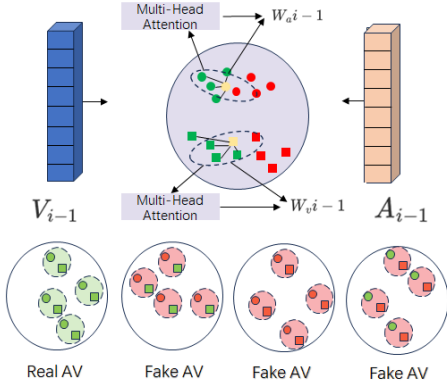


Figure 2: Adaptive Contrast Learning

define it as follows:

$$L_{av} = -\mathbb{E}_p(A,V)$$

$$\log \frac{\exp(\text{logits}_{\text{pos}_i})}{\exp(\text{logits}_{\text{pos}_i}) + \sum_{k=1}^K \exp(\text{logits}_{\text{neg}_{ik}})} \quad (2)$$

The logits for positive pairs are computed as: $\frac{S(x_{a_i}, x_{v_i})}{\tau}$ while those for negative pairs incorporate a margin m : $\frac{S(x_{a_i}, x_{v_k}^-)}{\tau} - \frac{m}{\tau}$.

For each pair of samples within a batch, we define their attention weights as:

$$w_{ij} = \frac{\exp(f_\theta(s_{ij}))}{\sum_{k,l} \exp(f_\theta(s_{kl}))} \quad (3)$$

Where f_θ represents a parameterized attention network that considers features such as the similarity value itself, deviation from the batch mean, and the distance between sample pairs in the feature space.

By integrating Bayesian estimation with the attention mechanism, we derive the updated formulation for the temperature parameter:

$$\tau = \tau_0 \cdot \exp\left(\sum_{k=1}^K \beta_k \phi_k(S)\right) \quad (4)$$

where $\phi_k(S)$ are a set of basis functions including: $\phi_1(S) = \text{Var}(S)$ (the variance term), $\phi_2(S) = \sum_{i,j} w_{ij} |s_{ij} - \mathbb{E}[S]|^3$ (weighted skewness), and $\phi_3(S) = H(w)$ (entropy of attention weights). The coefficients β_k are learnable parameters that combine these features.

A temporal adjustment factor is introduced to adapt the temperature parameter over time:

$$\gamma_t = \sigma(\text{MLP}([h_{t-1}, \Delta\tau_{t-1}, \text{grad}_\tau L_{t-1}])) \quad (5)$$

Consequently, the final temperature parameter at time t is defined as:

$$\tau_t = \gamma_t \cdot \tau_{t-1} + (1 - \gamma_t) \cdot \tau_{\text{new}} \quad (6)$$

where h_{t-1} encodes historical states, $\Delta\tau_{t-1}$ represents the temperature change from the previous step, and $\text{grad}_\tau L_{t-1}$ indicates the gradient of the loss with respect to the temperature. This approach leverages Bayesian inference for theoretical guarantees, captures fine-grained characteristics through the attention mechanism, and achieves temporal adaptation via dynamic adjustments.

Similarly, the contrastive loss from video to audio is formulated as:

$$L_{va} = -\mathbb{E}_p(V,A) \quad (7)$$

$$\sum_{i=1}^N \log \frac{\exp\left(\frac{\text{sim}(x_v^i, x_a^i)}{\tau}\right)}{\exp\left(\frac{\text{sim}(x_v^i, x_a^i)}{\tau}\right) + \sum_{k=1}^K \exp\left(\frac{\text{sim}(x_v^i, x_{a_k}^-)}{\tau} - m\right)}$$

where $x_{a_k}^-$ represents the queue of the nearest K negative audio samples not matching with video V .

Inspired by this, to preserve the efficacy of information within each single modality, we further implement intra-modality contrastive learning within both video and audio. We aggregate all losses into an adaptive modality contrastive learning loss as follows:

$$L_C = \frac{1}{4} [L_{va} + L_{av} + L_{vv} + L_{aa}], \quad (8)$$

where L_{vv} and L_{aa} denote the intra-modality contrastive losses for video and audio, respectively.

3.2.2 Adaptive Parameter Optimization for Contrastive Learning. Going further, as shown in Figure 2, we devise a weight parameter that guides the fusion of two modalities by exploiting the clustering information obtained after contrastive learning. This approach maximizes the utilization of latent information within each modality while optimizing the fusion strategy to enhance complementarity between modalities. As a result, the fused features more effectively represent the authenticity of samples.

We employ an adaptive clustering method that dynamically adjusts the number of clusters K based on data complexity. For video features $\{x_{v_i}\}$, we obtain cluster centers $\{c_v^k\}_{k=1}^K$; for audio features $\{x_{a_i}\}$, we obtain cluster centers $\{c_a^k\}_{k=1}^K$. Incorporating both Mahalanobis distance and cosine similarity, we propose a composite distance measure:

$$D_{v_i} = \beta \cdot \frac{d_{k_i}}{d_{\text{max}}^{k_i}} + (1 - \beta) \cdot s_{k_i} \quad (9)$$

where: $d_{k_i} = \sqrt{(x_{k_i} - c_{k_i})^\top \Sigma_k^{-1} (x_{k_i} - c_{k_i})}$, $s_{k_i} = 1 - \frac{x_{k_i}^\top c_{k_i}}{\|x_{k_i}\| \|c_{k_i}\|}$, $k \in \{a, v\}$, effectively measure the true distance between a sample and the cluster center, β is a balancing parameter, and $d_{\text{max}}^{k_i}$, $d_{\text{max}}^{a_i}$ are the maximum Mahalanobis distances in their respective modalities, used for normalization. The composite distance D_{v_i} captures both statistical distribution differences and directional discrepancies between samples and cluster centers. By introducing the balancing parameter β , we adjust the contributions of these two distances, thus obtaining a comprehensive evaluation of the relationship between samples and cluster centers. This enhanced distance metric improves clustering accuracy and provides a more reliable basis for modality fusion, thereby strengthening the representation of sample authenticity in the fused features.

Let $m \in \{v, a\}$ where v denotes the video modality and a the audio modality. We then apply a multi-head attention mechanism to comprehensively capture feature associations. Finally, we derive the importance scores:

$$w_{m_i} = \gamma \cdot \text{ReLU}(f_m(\text{MHAttention}_m)) + (1 - \gamma) \cdot \frac{1}{D_{m_i} + \epsilon} \quad (10)$$

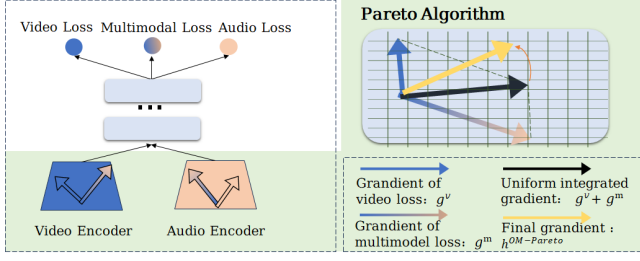


Figure 3: Orthogonalization-multimodal Pareto

where f_m is a learnable non-linear mapping function for modality m , $\gamma \in [0, 1]$ is a balance parameter controlling the weights of the attention output and distance measures.

3.2.3 Multi-Scale Feature Extraction. After encoding, audio and video yield feature representations V_i and A_i . Inspired by large-kernel convolutions, we design modality-specific feature extractors for video (V_{i-1}) and audio (A_{i-1}), capturing long-range dependencies and multi-scale information.

For video, the Multi-Scale Spatio-Temporal Large Kernel Attention (MSTLKA) block processes input features $H_v^{(L)} \in \mathbb{R}^{T \times C \times H \times W}$ as follows:

$$N = \text{LN}(H_v^{(L)}) \quad (11)$$

$$H_v^{(L)} = H_v^{(L)} + \lambda_1 f_3(\text{MSTLKA}(f_1(N)) \otimes f_2(N)) \quad (12)$$

$$N = \text{LN}(H_v^{(L)}) \quad (13)$$

$$H_v^{(L)} = H_v^{(L)} + \lambda_2 f_6(\text{GSAU-video}(f_4(N), f_5(N))) \quad (14)$$

Here, $f_i(\cdot)$ are 1×1 convolutions, and λ_1, λ_2 are learnable scalars. GSAU-video uses 3D depthwise convolutions for gating.

MSTLKA extends LKA to 3D convolutions for spatiotemporal dependencies. STLKA is:

$$\text{STLKA}(X) = f_{PW}(f_{DWD}(f_{DW}(X))) \quad (15)$$

where: f_{DW} : 3D depthwise convolution $(2d-1) \times (2d-1) \times (2d-1)$. f_{DWD} : 3D dilated depthwise convolution $\lceil \frac{K}{d} \rceil$. f_{PW} : Pointwise convolution.

Input features are split into n groups, and MSTLKA is applied at different scales:

$$\text{MSTLKA}_i(X_i) = G_i(X_i) \otimes \text{STLKA}_i(X_i) \quad (16)$$

$G_i(\cdot)$ is a 3D depthwise convolution gating mechanism, dynamically adjusting attention.

The audio pathway shares the same structure as video but employs 2D operations for time-frequency modeling, with MSTLKA replaced by MFTLKA and GSAU simplified to 2D.

3.2.4 Multimodal Feature Fusion. Utilizing the computed fusion weights, we perform a weighted fusion of deep video and audio features to obtain a fused feature representation. Specifically, the calculation for the fused feature x_{fused_i} is defined as:

$$x_{\text{fused}_i} = w_{v_i} \cdot V_{i-1} + w_{a_i} \cdot A_{i-1} \quad (17)$$

In this equation, w_{v_i} and w_{a_i} denote the fusion weights for the video and audio modalities, respectively, while V_{i-1} and A_{i-1} represent

the deep features from the video and audio streams at the previous layer.

By employing this method, we effectively integrate information from both video and audio modalities, leveraging their complementary nature to enhance the model's capability in representing multimodal data. Subsequently, using x_{fused_i} —which encapsulates global audio-video fusion information—we guide the learning of complementary modality information and global context in deeper layers:

$$K_i = K'_{i-1} \otimes x_{\text{fused}_i} \quad K \in \{V, A\} \quad (18)$$

3.3 Representation Fusion via Multi-Head Attention Framework

After multi-scale feature fusion, the audio and video modalities are represented as $\{ha_i, hv_i \dots ha_{i+n}, hv_{i+n}\}$, which are fused into a joint vector for deepfake detection. Our fusion mechanism employs a Transformer-based self-attention framework: $\text{head}_i = \text{Attention}(Q W_i^q, K W_i^k, V W_i^v)$. Stack the representations into matrix $M = [ha_i, hv_i \dots ha_{i+n}, hv_{i+n}]$ and process through multi-head attention: $M = (\text{head}_1 \oplus \dots \oplus \text{head}_n) W^o$ where Θ_{att} denotes attention parameters and W^o is the output transformation matrix. This enables cross-modal interaction through multiple attention heads, producing enriched features M for detection.

3.4 Classify

The classification module operates at both frame-level and sample-level granularity.

Utilizing the fused feature matrix M output by the RFMF module, an MLP is designed for authenticity discrimination. The model adopts a progressive dimensionality reduction architecture: stacked fully connected layers gradually compress feature dimensions, step-wise abstracting discriminative high-level semantic representations. Between network layers, a hybrid integration of BatchNorm and Dropout layers implements dual regularization — standardizing feature distributions through BatchNorm while randomly deactivating neurons via Dropout — thereby mitigating the risk of overfitting. The final layer employs the Sigmoid function to map features into the $[0, 1]$ interval, outputting the estimated probability of a sample being forged. The training process utilizes the binary cross-entropy loss function:

$$\mathcal{L}_{\text{sample}}^k = -\frac{1}{N} \sum_{i=1}^N [y_i \log \hat{y}_i + (1 - y_i) \log(1 - \hat{y}_i)] \quad (19)$$

where $k \in \{\text{audio}, \text{video}\}$, $y_i \in \{0, 1\}$ denotes the ground-truth label and \hat{y}_i represents the predicted probability.

For each temporal frame t in feature after Multi-Scale Feature Fusion With Contrastive Learning, independent MLP branches process audio/video features:

$$\mathcal{L}_{\text{frame}}^k = -\frac{1}{N} \sum_{i=1}^N [y_i \log \hat{y}_i + (1 - y_i) \log(1 - \hat{y}_i)] \quad (20)$$

where $k \in \{\text{audio}, \text{video}\}$.

Table 1: COMPARISON WITH OTHER METHODS ON INTRA-DATASETS USING SAMPLE-LEVEL AUC AND ACC METRICS

Methods	Modality	DefakeAVMiT		FakeAVCeleb		DFDC		Avg	
		ACC(%)	AUC(%)	ACC(%)	AUC(%)	ACC(%)	AUC(%)	ACC(%)	AUC(%)
Multiple-Attention [43] (2021)	visual	85.1	87.3	77.6	79.3	82.5	84.8	81.7	83.8
SLADD [5] (2022)	visual	73.3	77.5	70.5	72.1	73.6	75.2	72.5	74.9
ECAPA-TDNN [9] (2020)	audio	70.2	72.6	59.8	62.7	67.3	69.8	65.8	68.4
AASIST [17] (2021)	audio	67.5	69.8	53.4	55.1	64.8	68.4	61.9	64.4
AVFakeNet [16] (2022)	audio-visual	91.8	93.7	78.4	83.4	82.8	86.2	84.3	87.8
VFD [6] (2022)	audio-visual	93.4	95.6	81.5	86.1	80.9	85.1	85.3	88.9
BA-TFD [3] (2022)	audio-visual	92.1	94.9	80.8	84.9	79.1	84.6	84.0	88.1
AVoiD-DF [40] (2023)	audio-visual	95.3	97.6	83.7	89.2	91.4	94.8	90.1	93.9
MCL [23] (2024)	audio-visual	-	-	85.9	89.2	97.5	98.3	91.7	93.8
MACB-DF (Ours)	audio-visual	96.8	98.7	91.7	93.2	97.9	98.8	95.5	96.9

3.5 Orthogonalization-multimodal Pareto

consider the following constrained optimization problem:

$$\begin{aligned}
 \min_{\alpha_m, \alpha_u} \quad & \mathcal{L}_0 = \|\alpha_m \mathbf{g}_m + \alpha_u \mathbf{g}_u\|^2 \\
 \text{s.t.} \quad & \alpha_m + \alpha_u = 1 \\
 & \alpha_m, \alpha_u \geq 0
 \end{aligned} \quad (21)$$

where $\mathbf{g}_m \in \mathbb{R}^d$ and $\mathbf{g}_u \in \mathbb{R}^d$ represent multimodal and unimodal gradient vectors, respectively.

An implicit orthogonal regularization term is introduced during gradient updates to construct augmented gradients:

$$\nabla_{\alpha} \mathcal{L}_{\text{aug}} = \nabla_{\alpha} \mathcal{L}_0 + \lambda_{\text{orth}} \cdot \nabla_{\alpha} (\alpha_m \alpha_u |\mathbf{g}_m^{\top} \mathbf{g}_u|) \quad (22)$$

The regularization strength parameter is adaptively adjusted based on gradient directional similarity:

$$\lambda_{\text{orth}} = \frac{\lambda_0}{1 + \exp(\kappa \cos \theta)}, \quad \cos \theta = \frac{\mathbf{g}_m^{\top} \mathbf{g}_u}{\|\mathbf{g}_m\| \|\mathbf{g}_u\|} \quad (23)$$

where $\kappa > 0$ denotes the curvature control parameter and λ_0 represents the baseline regularization strength.

Non-Conflict Scenario ($\cos \theta \geq 0$)

- Maintain original Pareto uniform weighting: $\alpha_m = \alpha_u = 0.5$
- Apply mild orthogonal correction: $\lambda_{\text{orth}} \leftarrow 0.1\lambda_0$

Conflict Scenario ($\cos \theta < 0$)

- Execute complete PGD iterations
- Noise-amplified gradient magnitude:

$$\mathbf{h}_{\text{final}} = \frac{\alpha_m^* \mathbf{g}_m + \alpha_u^* \mathbf{g}_u}{\|\alpha_m^* \mathbf{g}_m + \alpha_u^* \mathbf{g}_u\|} \cdot \left(1 + \frac{|\cos \theta|}{1 + \|\mathbf{g}_m\|/\|\mathbf{g}_u\|}\right) \|\mathbf{g}_m + \mathbf{g}_u\| \quad (24)$$

4 EXPERIMENTS

4.1 Datasets

DefakeAVMiT This multimodal dataset [40] contains 6,480 audiovisual samples generated using 8 distinct deepfake methods. It features four combinatorial classes: $\mathbf{V_R A_R}$: Real visual/audio, $\mathbf{V_F A_R}$, $\mathbf{V_R A_F}$, $\mathbf{V_F A_F}$: Hybrid/fake combinations. Samples are temporally aligned to ensure audiovisual synchronization.

FakeAVCeleb Derived from VoxCeleb2, this benchmark [18] expands 490 real videos to 19,500 synthetic samples using Visual

Table 2: ABLATION STUDY ON CONTRASTIVE LEARNING

Methods	FakeAVCeleb		DFDC	
	ACC(%)	AUC(%)	ACC(%)	AUC(%)
MACB-DF w/o L_C	88.5	90.2	93.2	95.1
MACB-DF w/o L_{intra}	90.1	92.2	95.5	96.8
MACB-DF w/o L_{cross}	90.9	92.8	96.9	97.2
MACB-DF w/o w	91.2	92.8	97.3	98.4
MACB-DF	91.7	93.2	97.9	98.8

manipulation: Faceswap/FSGAN, Audiovisual synthesis: SV2TTS/Wav2Lip. Emphasizes lip-synced audio-visual coherence through frame-level alignment.

DFDC This large-scale dataset [10] contains >100k clips from 3,426 subjects featuring: Multi-method visual forgery (DFAE, StyleGAN, etc.), Single-mode audio synthesis (TTS Skins). Notably lacks lip-sync between synthetic audio and visual frames.

LAV-DF This large-scale dataset [3] contains 136,304 videos featuring 153 unique identities, with 36,431 completely real videos and 99,873 videos containing fake segments. The dataset is tasks with per-frame authenticity labels.

4.2 Performance

4.2.1 sample-level detection performance. This section evaluates our framework’s sample-level detection performance across all training datasets. For rigorous validation, we compare Deepfake detection methods: video-based approaches [5, 43], audio-centric methods [9, 17], and multimodal fusion techniques [3, 6, 16, 23, 40]. Datasets were partitioned using randomized stratification (80:20 train-test ratio) to ensure unbiased evaluation.

As shown in Table 1, MACB-DF demonstrates consistently strong performance across all evaluated datasets. On DefakeAVMiT, it attains 96.8% ACC and 98.7% AUC, surpassing existing methods by a significant margin. For FakeAVCeleb, which features diverse Deepfake variants, MACB-DF demonstrates exceptional performance

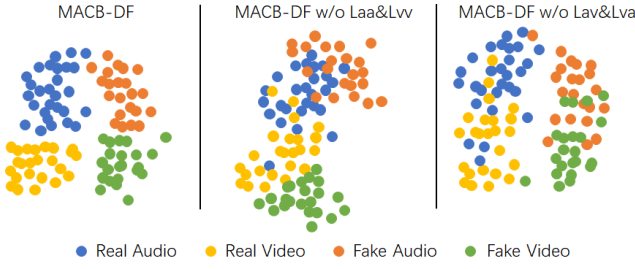


Figure 4: Ablation Study on Contrastive Learning: Latent Space Visualization

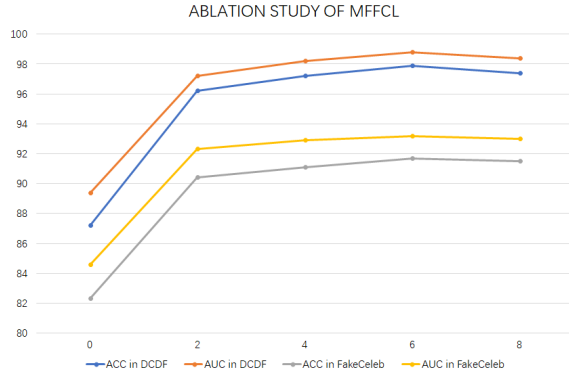


Figure 5: Ablation Study on MFFCL: Impact on AUC/ACC Metrics for DFDC and FakeAVCeleb Datasets

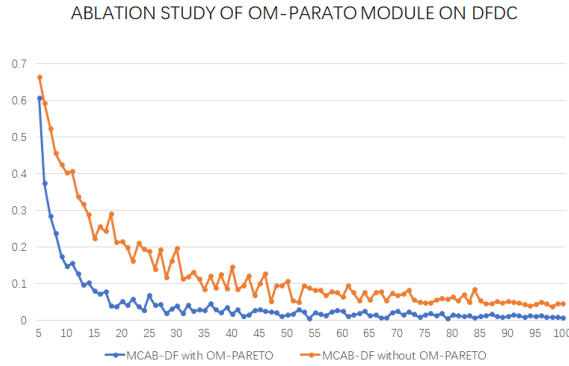


Figure 6: Ablation Study on OM-Pareto: Impact of Loss Function

with 91.7% ACC and 93.2% AUC, achieving substantial improvements over prior approaches. On the challenging DFDC dataset, MACB-DF achieves 97.9% ACC and 98.8% AUC. Across all datasets, MACB-DF achieves an average of 95.5% ACC and 96.9% AUC, significantly outperforming other state-of-the-art methods. Three key innovations drive this advancement: 1) **Contrastive Multimodal Alignment**: Reduces biased dominance and information conflicts

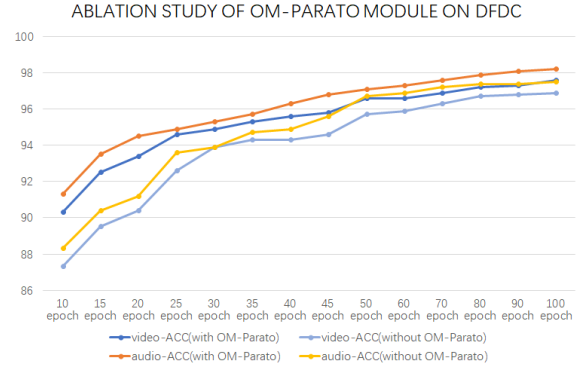


Figure 7: Ablation Study of OM-Pareto: Impact on Video and Audio AUC/ACC Metrics

during fusion through contrastive learning; 2) **Hierarchical Feature Extraction**: Combines global context with deep local patterns through multi-scale architecture.

5 ABLATION STUDY

5.1 Contrastive Learning

To validate the contribution of contrastive learning, we analyze four variants of our MACB-DF framework with results in Table 2: 1) MACB-DF w/o L_C : Exclusion of contrastive learning mechanisms (ACC drops by 3.2%/4.7% on FakeAVCeleb/DFDC compared to full model), 2) MACB-DF w/o L_{intra} : Ablation of contrastive loss L_{aa} and L_{vv} (AUC decreases 1.0%/2.0% demonstrating modality-specific alignment necessity), 3) MACB-DF w/o L_{cross} : Ablation of contrastive loss L_{av} and L_{va} (ACC gap of 0.8%/1.0% highlights cross-modal synchronization value), 4) MACB-DF w/o w : Removal of adaptive fusion weighting (97.3% \rightarrow 97.9% ACC on DFDC proves dynamic weighting superiority). The latent space visualization of ablation study on contrastive learning is shown in Figure 4. The empirical findings substantiate that contrastive learning significantly enhances discriminative capacity through three synergistic effects: 1) **Inter-modal Discrepancy Learning**: Intra- and cross-modal contrastive learning enables comprehensive exploitation of inter-modal discrepancies, particularly effective for detecting subtle audio-visual asynchrony, 2) **Representation Polarization**: The push-pull dynamics between positive pairs (intra-class) and negative pairs (inter-class) amplify decision boundaries by a% compared to baseline models, 3) **Cluster-aware Fusion**: Cluster density-based weighting automatically balances modality-specific contributions.

5.2 Multi-Scale Feature Fusion With Contrastive Learning

We conducted experiments with five different depths of deep feature extraction layers (0, 2, 4, 6, 8) on the DFDC dataset and FakeAVCeleb dataset. The results are shown in Figure 5. As the number of layers increases, the accuracy first improves and then slightly declines. Notably, the accuracy peaks at six layers, achieving an ACC of 97.9% on the DFDC dataset and 91.7% on the FakeAVCeleb dataset.

Table 3: THE ACCS OF CROSS-DATASET EXPERIMENTS. THE TRAINING SETS AND TESTING SETS FOR CROSS-DATASET

Methods	DFDC	
	DefakeAVMiT	FakeAVCeleb
CViT	47.2	45.5
MesoNet	57.7	54.1
MDS	76.5	72.9
AVoiD-DF	84.4	82.8
MACB-DF	91.2	89.2

A potential explanation for this phenomenon is that an appropriate number of layers allows the model to effectively fuse deep-level features with global features, thereby enhancing the learning of multimodal information. However, excessive layers may lead to the loss of critical information during the extraction process, resulting in reduced accuracy.

5.3 Orthogonalization-multimodal Pareto

For the orthogonalization-multimodal pareto module, its primary function lies in mitigating multi-modal gradient conflicts. To validate this, we evaluate the model accuracy with and without the module across different training epochs, as illustrated in Figure 6 and Figure 7. The experimental results demonstrate that during the early training stages with fewer epochs, the model equipped with the orthogonalization-multimodal pareto module exhibits a significantly faster loss reduction rate and a more stable convergence trajectory. Moreover, the accuracy of the orthogonalization-multimodal pareto model substantially outperforms its counterpart without the module across both video and audio modalities. Notably, the performance hole gradually diminishes as the number of training epochs increases. These observations conclusively substantiate that our proposed Pareto module effectively alleviates gradient conflicts, thereby facilitating more efficient learning of multi-modal representations during the critical initial training phases.

6 GENERALIZATION TESTS

The cross-dataset generalization capability of our method is comprehensively evaluated through rigorous experiments, as shown in Table 3. When trained on DFDC and tested on DefakeAVMiT and FakeAVCeleb datasets, MACB-DF achieves remarkable ACC scores of 91.2% and 89.2% respectively, significantly outperforming existing state-of-the-art methods. Notably, our approach demonstrates 6.8% and 6.4% absolute improvements over the previous best method (AVoiD-DF) on two testing sets, revealing superior adaptability to unknown data distributions. This enhanced generalization stems from our balanced multimodal fusion strategy and effective mitigation of modality bias, which prevents overfitting to dataset-specific artifacts.

7 CONCLUSION

We propose MACB-DF, a novel audio-visual joint learning framework for multimedia deepfake detection that addresses modality

bias and gradient conflicts in multimodal fusion. By integrating hierarchical contrastive learning with authenticity-aware adaptation, MACB-DF achieves balanced cross-modal representation while preserving fine-grained unimodal features. The Pareto module further resolves optimization conflicts, enhancing robustness and complementarity. Extensive experiments demonstrate state-of-the-art performance on benchmark datasets, with significant improvements in cross-dataset generalization. These results underscore MACB-DF's effectiveness in critical multimedia applications such as cybersecurity, content authentication, and media review systems. Future work will explore lightweight deployment strategies and temporal consistency modeling to enhance scalability and real-time applicability in dynamic multimedia environments.

8 ACKNOWLEDGMENTS

This work was supported by the National Natural Science Foundation of China(62471090), Sichuan Provincial Natural Science Foundation Project(23NSFSC0422), Central University Fund(ZYGX2024Z016).

References

- [1] Tadas Baltrušaitis, Chaitanya Ahuja, and Louis-Philippe Morency. 2019. Multimodal Machine Learning: A Survey and Taxonomy. *IEEE Transactions on Pattern Analysis and Machine Intelligence* 41, 2 (2019), 423–443. doi:10.1109/TPAMI.2018.2798607
- [2] Remi Cadene, Corentin Dancette, Matthieu Cord, Devi Parikh, et al. 2019. Rubi: Reducing unimodal biases for visual question answering. *Advances in neural information processing systems* 32 (2019).
- [3] Zhixi Cai, Kalin Stefanov, Abhinav Dhall, and Munawar Hayat. 2022. Do you really mean that? content driven audio-visual deepfake dataset and multimodal method for temporal forgery localization. In *2022 International Conference on Digital Image Computing: Techniques and Applications (DICTA)*. IEEE, IEEE, 1–10.
- [4] Caroline Chan, Shiry Ginosar, Tinghui Zhou, and Alexei A Efros. 2019. Everybody dance now. In *Proceedings of the IEEE/CVF international conference on computer vision*. 5933–5942.
- [5] Liang Chen, Yong Zhang, Yibing Song, Lingqiao Liu, and Jue Wang. 2022. Self-supervised Learning of Adversarial Example: Towards Good Generalizations for Deepfake Detection. In *2022 IEEE/CVF Conference on Computer Vision and Pattern Recognition (CVPR)*. 18689–18698. doi:10.1109/CVPR52688.2022.01815
- [6] Harry Cheng, Yangyang Guo, Tianyi Wang, Qi Li, Xiaojun Chang, and Liqiang Nie. 2023. Voice-face homogeneity tells deepfake. *ACM Transactions on Multimedia Computing, Communications and Applications* 20, 3 (2023), 1–22.
- [7] Komal Chugh, Parul Gupta, Abhinav Dhall, and Ramanathan Subramanian. 2020. Not made for each other-audio-visual dissonance-based deepfake detection and localization. In *Proceedings of the 28th ACM international conference on multimedia*. 439–447.
- [8] Hao Dang, Feng Liu, Joel Stehouwer, Xiaoming Liu, and Anil K. Jain. 2020. On the Detection of Digital Face Manipulation. In *Proceedings of the IEEE/CVF Conference on Computer Vision and Pattern Recognition (CVPR)*.
- [9] Brecht Desplanques, Jenthe Thienpondt, and Kris Demuyne. 2020. Ecapt-dnn: Emphasized channel attention, propagation and aggregation in tdn based speaker verification. *arXiv preprint arXiv:2005.07143*.
- [10] Brian Dolhansky, Joanna Bitton, Ben Pfau, Jikuo Lu, Russ Howes, Menglin Wang, and Cristian Canton Ferrer. 2020. The deepfake detection challenge (dfdc) dataset. *arXiv preprint arXiv:2006.07397* (2020).
- [11] Tharindu Fernando, Clinton Fookes, Simon Denman, and Sridha Sridharan. 2019. Exploiting human social cognition for the detection of fake and fraudulent faces via memory networks. *arXiv preprint arXiv:1911.07844* (2019).
- [12] Qiqi Gu, Shen Chen, Taiping Yao, Yang Chen, Shouhong Ding, and Ran Yi. 2022. Exploiting fine-grained face forgery clues via progressive enhancement learning. In *Proceedings of the AAAI Conference on Artificial Intelligence*, Vol. 36. 735–743.
- [13] Ruidong Han, Xiaofeng Wang, Ningning Bai, Qin Wang, Zinian Liu, and Jianru Xue. 2023. FCD-Net: Learning to detect multiple types of homologous deepfake face images. *IEEE Transactions on Information Forensics and Security* 18 (2023), 2653–2666.
- [14] Peisong He, Haoliang Li, and Hongxia Wang. 2019. Detection of fake images via the ensemble of deep representations from multi color spaces. In *2019 IEEE international conference on image processing (ICIP)*. IEEE, 2299–2303.
- [15] R Huang, MWY Lam, J Wang, D Su, D Yu, Y Ren, and Z Zhao. 2022. FastDiff: A Fast Conditional Diffusion Model for High-Quality Speech Synthesis. In *IJCAI*

- International Joint Conference on Artificial Intelligence*. IJCAI: International Joint Conferences on Artificial Intelligence Organization, 4157–4163.
- [16] Hafsa Ilyas, Ali Javed, and Khalid Mahmood Malik. 2023. AVFakeNet: A unified end-to-end Dense Swin Transformer deep learning model for audio-visual deepfakes detection. *Applied Soft Computing* 136 (2023), 110124.
 - [17] Jee-weon Jung, Hee-Soo Heo, Hemlata Tak, Hye-jin Shim, Joon Son Chung, Bong-Jin Lee, Ha-Jin Yu, and Nicholas Evans. 2022. Aasist: Audio anti-spoofing using integrated spectro-temporal graph attention networks. In *ICASSP 2022-2022 IEEE international conference on acoustics, speech and signal processing (ICASSP)*. IEEE, 6367–6371.
 - [18] Hasam Khalid, Shahroz Tariq, Minha Kim, and Simon S Woo. 2021. FakeAVCeleb: A novel audio-video multimodal deepfake dataset. *arXiv preprint arXiv:2108.05080* (2021).
 - [19] Lingzhi Li, Jianmin Bao, Hao Yang, Dong Chen, and Fang Wen. 2020. Advancing high fidelity identity swapping for forgery detection. In *Proceedings of the IEEE/CVF conference on computer vision and pattern recognition*. 5074–5083.
 - [20] Yuanman Li and Jiantao Zhou. 2018. Fast and effective image copy-move forgery detection via hierarchical feature point matching. *IEEE Transactions on Information Forensics and Security* 14, 5 (2018), 1307–1322.
 - [21] Paul Pu Liang, Amir Zadeh, and Louis-Philippe Morency. 2024. Foundations & trends in multimodal machine learning: Principles, challenges, and open questions. *Comput. Surveys* 56, 10 (2024), 1–42.
 - [22] T Lin. 2017. Focal Loss for Dense Object Detection. *arXiv preprint arXiv:1708.02002* (2017).
 - [23] Xiaolong Liu, Yang Yu, Xiaolong Li, and Yao Zhao. 2024. MCL: Multimodal Contrastive Learning for Deepfake Detection. *IEEE Transactions on Circuits and Systems for Video Technology* 34, 4 (2024), 2803–2813. doi:10.1109/TCSVT.2023.3312738
 - [24] Dhruv Malik, Ashwin Pananjady, Kush Bhatia, Koulik Khamaru, Peter I Bartlett, and Martin J Wainwright. 2020. Derivative-free methods for policy optimization: Guarantees for linear quadratic systems. *Journal of Machine Learning Research* 21, 21 (2020), 1–51.
 - [25] Fatemeh Zare Mehrjardi, Ali Mohammad Latif, Mohsen Sardari Zarchi, and Razieh Sheikhpour. 2023. A survey on deep learning-based image forgery detection. *Pattern Recognition* (2023), 109778.
 - [26] Trisha Mittal, Uttaran Bhattacharya, Rohan Chandra, Aniket Bera, and Dinesh Manocha. 2020. Emotions don't lie: An audio-visual deepfake detection method using affective cues. In *Proceedings of the 28th ACM international conference on multimedia*. 2823–2832.
 - [27] Huy H Nguyen, Junichi Yamagishi, and Isao Echizen. 2019. Capsule-forensics: Using capsule networks to detect forged images and videos. In *ICASSP 2019-2019 IEEE international conference on acoustics, speech and signal processing (ICASSP)*. IEEE, 2307–2311.
 - [28] Fan Nie, Jiangqun Ni, Jian Zhang, Bin Zhang, and Weizhe Zhang. 2024. FRADE: Forgery-aware Audio-distilled Multimodal Learning for Deepfake Detection. In *Proceedings of the 32nd ACM International Conference on Multimedia*. 6297–6306.
 - [29] Xiaokang Peng, Yake Wei, Andong Deng, Dong Wang, and Di Hu. 2022. Balanced multimodal learning via on-the-fly gradient modulation. In *Proceedings of the IEEE/CVF conference on computer vision and pattern recognition*. 8238–8247.
 - [30] Jinghan Ru, Jun Tian, Chengwei Xiao, Jingjing Li, and Heng Tao Shen. 2024. Imbalanced Open Set Domain Adaptation via Moving-Threshold Estimation and Gradual Alignment. *IEEE Transactions on Multimedia* 26 (2024), 2504–2514. doi:10.1109/TMM.2023.3297768
 - [31] Jinghan Ru, Yuxin Xie, Xianwei Zhuang, Yuguo Yin, and Yuexian Zou. 2025. Do we really have to filter out random noise in pre-training data for language models? *arXiv:2502.06604* [cs.CL] <https://arxiv.org/abs/2502.06604>
 - [32] Ekraam Sabir, Jiaxin Cheng, Ayush Jaiswal, Wael AbdAlmageed, Iacopo Masi, and Prem Natarajan. 2019. Recurrent convolutional strategies for face manipulation detection in videos. *Interfaces (GUI)* 3, 1 (2019), 80–87.
 - [33] Sanait Javid Sohrawardi, Akash Chinttha, Bao Thai, Sovanharith Seng, Andrea Hickerson, Raymond Ptucha, and Matthew Wright. 2019. Poster: Towards robust open-world detection of deepfakes. In *Proceedings of the 2019 ACM SIGSAC conference on computer and communications security*. 2613–2615.
 - [34] Shahroz Tariq, Sangyup Lee, Hoyoung Kim, Youjin Shin, and Simon S Woo. 2018. Detecting both machine and human created fake face images in the wild. In *Proceedings of the 2nd international workshop on multimedia privacy and security*. 81–87.
 - [35] Shahroz Tariq, Sangyup Lee, Hoyoung Kim, Youjin Shin, and Simon S Woo. 2019. Gan is a friend or foe? a framework to detect various fake face images. In *Proceedings of the 34th ACM/SIGAPP Symposium on Applied Computing*. 1296–1303.
 - [36] Weiyao Wang, Du Tran, and Matt Feiszli. 2020. What makes training multimodal classification networks hard?. In *Proceedings of the IEEE/CVF conference on computer vision and pattern recognition*. 12695–12705.
 - [37] Yaohui Wang, Piotr Bilinski, Francois Bremond, and Antitza Dantcheva. 2020. Imaginator: Conditional spatio-temporal gan for video generation. In *Proceedings of the IEEE/CVF Winter Conference on Applications of Computer Vision*. 1160–1169.
 - [38] Nan Wu, Stanislaw Jastrzebski, Kyunghyun Cho, and Krzysztof J Geras. 2022. Characterizing and overcoming the greedy nature of learning in multi-modal deep neural networks. In *International Conference on Machine Learning*. PMLR, 24043–24055.
 - [39] Yuxin Xie, Zhihong Zhu, Xianwei Zhuang, Liming Liang, Zhichang Wang, and Yuexian Zou. 2024. GPA: Global and Prototype Alignment for Audio-Text Retrieval. In *Interspeech 2024*. 5078–5082. doi:10.21437/Interspeech.2024-1642
 - [40] Wenyuan Yang, Xiaoyu Zhou, Zhikai Chen, Bofei Guo, Zhongjie Ba, Zhihua Xia, Xiaochun Cao, and Kui Ren. 2023. AVoid-DF: Audio-Visual Joint Learning for Detecting Deepfake. *IEEE Transactions on Information Forensics and Security* 18 (2023), 2015–2029. doi:10.1109/TIFS.2023.3262148
 - [41] Yuguo Yin, Yuxin Xie, Wenyuan Yang, Dongchao Yang, Jinghan Ru, Xianwei Zhuang, Liming Liang, and Yuexian Zou. 2025. ATRI: Mitigating Multilingual Audio Text Retrieval Inconsistencies by Reducing Data Distribution Errors. *arXiv:2502.14627* [cs.SD] <https://arxiv.org/abs/2502.14627>
 - [42] Yang Yu, Xiaolong Liu, Rongrong Ni, Siyuan Yang, Yao Zhao, and Alex C. Kot. 2024. PVASS-MDD: Predictive Visual-Audio Alignment Self-Supervision for Multimodal Deepfake Detection. *IEEE Transactions on Circuits and Systems for Video Technology* 34, 8 (2024), 6926–6936. doi:10.1109/TCSVT.2023.3309899
 - [43] Hanqing Zhao, Wenbo Zhou, Dongdong Chen, Tianyi Wei, Weiming Zhang, and Nenghai Yu. 2021. Multi-attentional Deepfake Detection. *arXiv:2103.02406* [cs.CV] <https://arxiv.org/abs/2103.02406>
 - [44] Tianfei Zhou, Wenguan Wang, Zhiyuan Liang, and Jianbing Shen. 2021. Face forensics in the wild. In *Proceedings of the IEEE/CVF conference on computer vision and pattern recognition*. 5778–5788.
 - [45] Xianwei Zhuang, Hongxiang Li, Yuxin Cheng, Zhihong Zhu, Yuxin Xie, and Yuexian Zou. 2025. KDProR: A Knowledge-Decoupling Probabilistic Framework for Video-Text Retrieval. In *Computer Vision – ECCV 2024*, Aleš Leonardis, Elisa Ricci, Stefan Roth, Olga Russakovsky, Torsten Sattler, and Gül Varol (Eds.). Springer Nature Switzerland, Cham, 313–331.
 - [46] Xianwei Zhuang, Yuxin Xie, Yufan Deng, Dongchao Yang, Liming Liang, Jinghan Ru, Yuguo Yin, and Yuexian Zou. 2025. VARGPT-v1.1: Improve Visual Autoregressive Large Unified Model via Iterative Instruction Tuning and Reinforcement Learning. *arXiv:2504.02949* [cs.CV] <https://arxiv.org/abs/2504.02949>
 - [47] Xianwei Zhuang, Zhihong Zhu, Yuxin Xie, Liming Liang, and Yuexian Zou. 2025. VASparse: Towards Efficient Visual Hallucination Mitigation via Visual-Aware Token Sparsification. *arXiv:2501.06553* [cs.CV] <https://arxiv.org/abs/2501.06553>